# Electronic Supplementary Material

## Bamboo-like *N*-doped carbon nanotubes encapsulating M(Co, Fe)-Ni alloy for electrochemical production of syngas with potential-independent $CO/H_2$ ratios

**Jinxiao Bo[1], Mei Li[1], Xinli Zhu[1], Qingfeng Ge[2], Jinyu Han[1], Hua Wang (✉)[1]**

1 Key Laboratory for Green Chemical Technology of Ministry of Education, Collaborative Innovation Center of Chemical Science and Engineering, School of Chemical Engineering and Technology, Tianjin University, Tianjin 300072, China

2 Department of Chemistry and Biochemistry, Southern Illinois University, Carbondale, IL 62901, USA

E-mail: tjuwanghua@tju.edu.cn

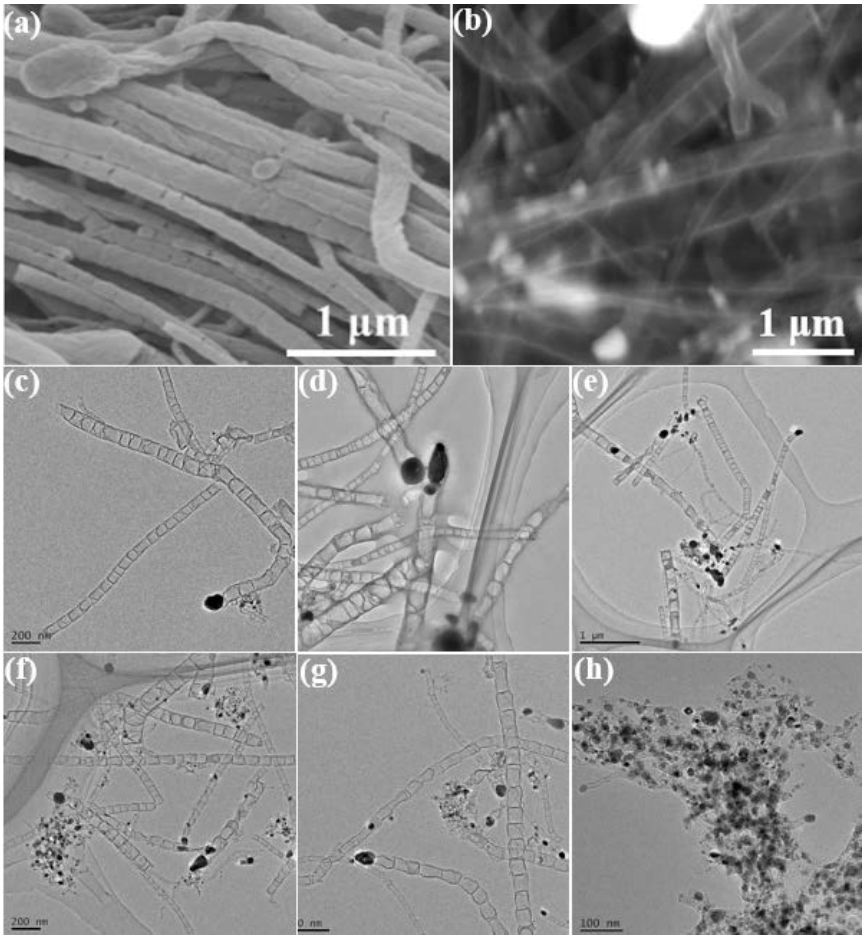


**Fig. S1** SEM images of (a) Ni-NCNT, (b) Co-NCNT; TEM images of (c) Co-NCNT, (d) Ni-NCNT, (e) $Co_2Ni$-NCNT, (f) $Fe_1Ni$-NCNT, (g) $Fe_2Ni$-NCNT and (h) Fe-NCNT

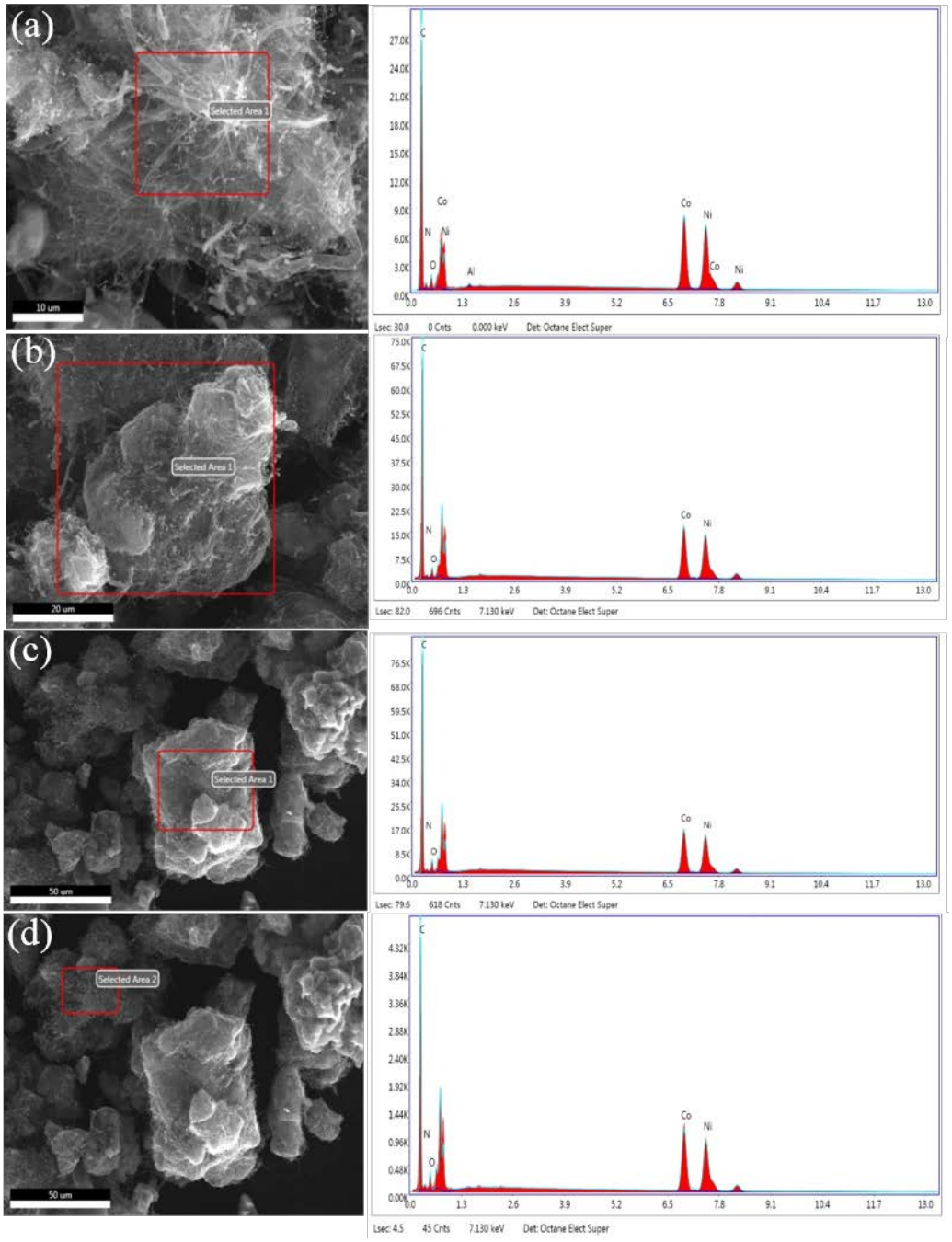


**Fig. S2** SEM images and compositions by SEM-EDS of $Co_1Ni$-NCNT

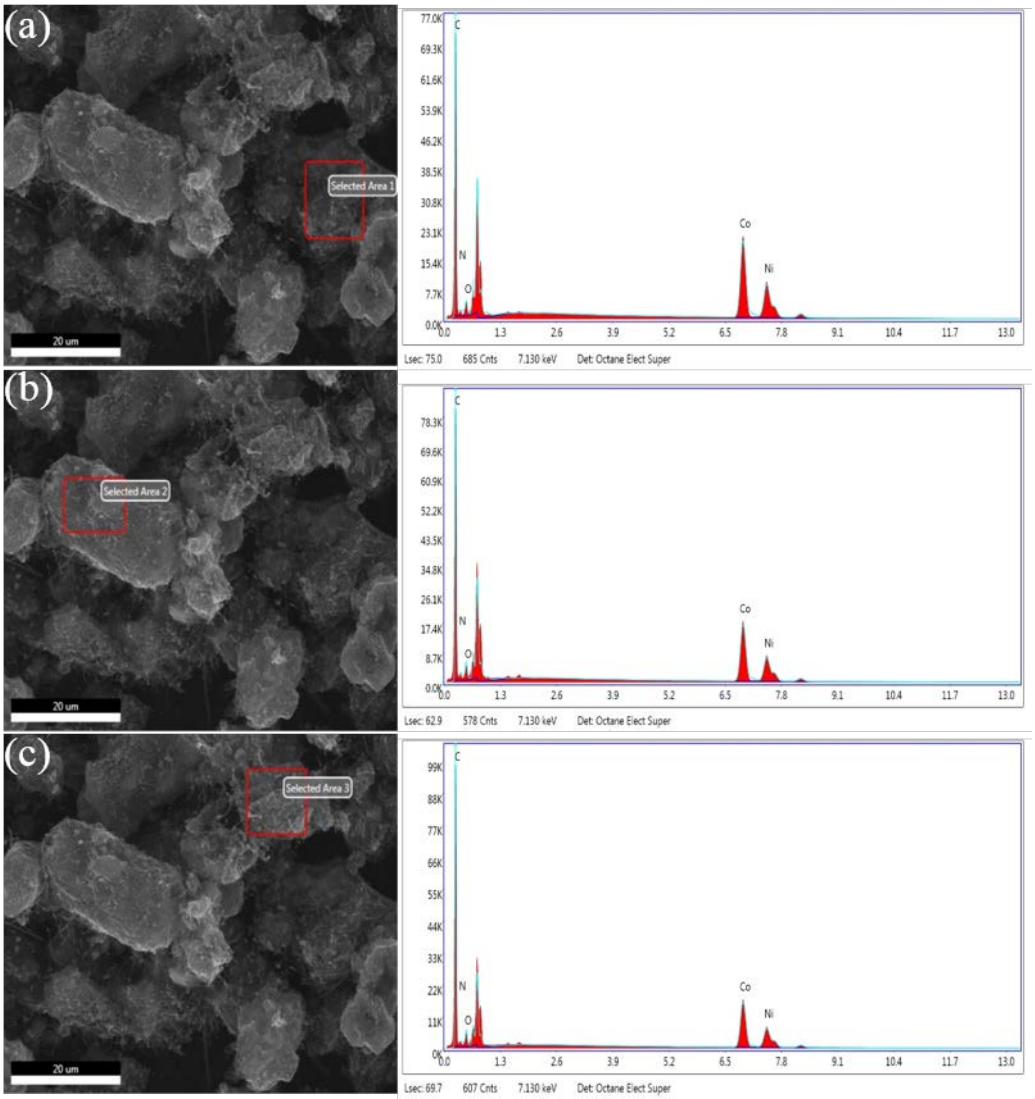


**Fig. S3** SEM images and compositions by SEM-EDS of $Co_2Ni$-NCNT

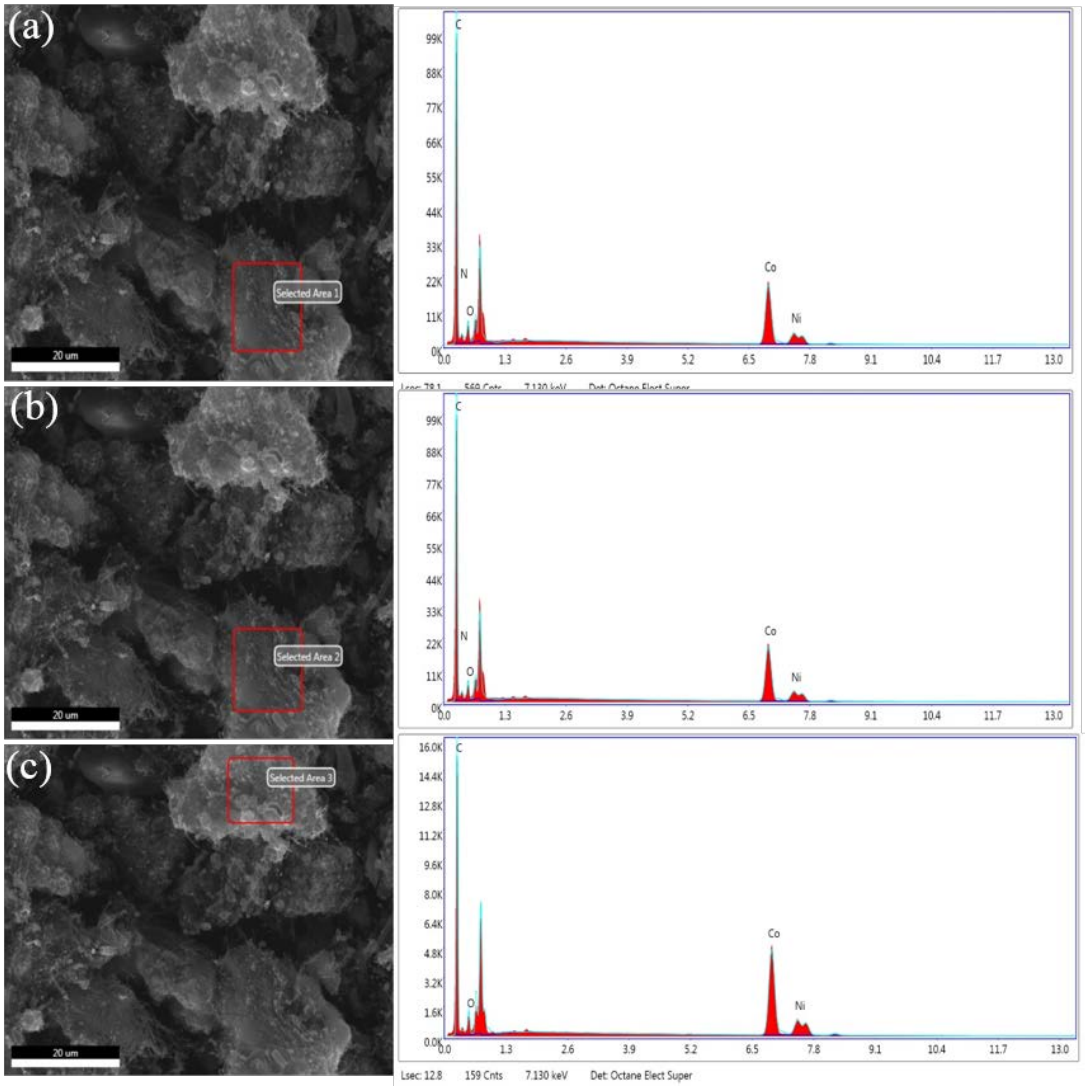


**Fig. S4** SEM images and compositions by SEM-EDS of $Co_5Ni$-NCNT

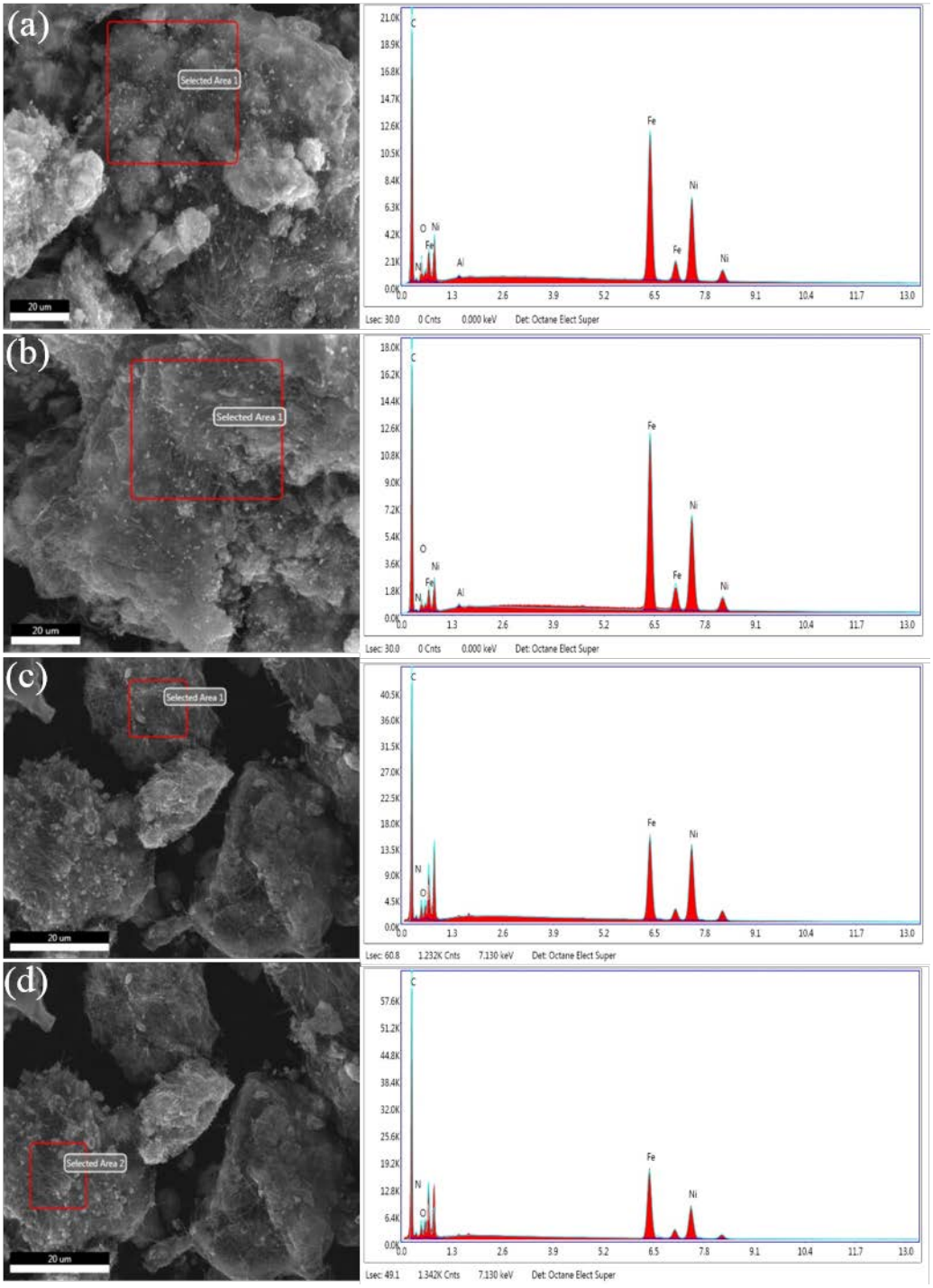


**Fig. S5** SEM images and compositions by SEM-EDS of $Fe_1Ni$-NCNT

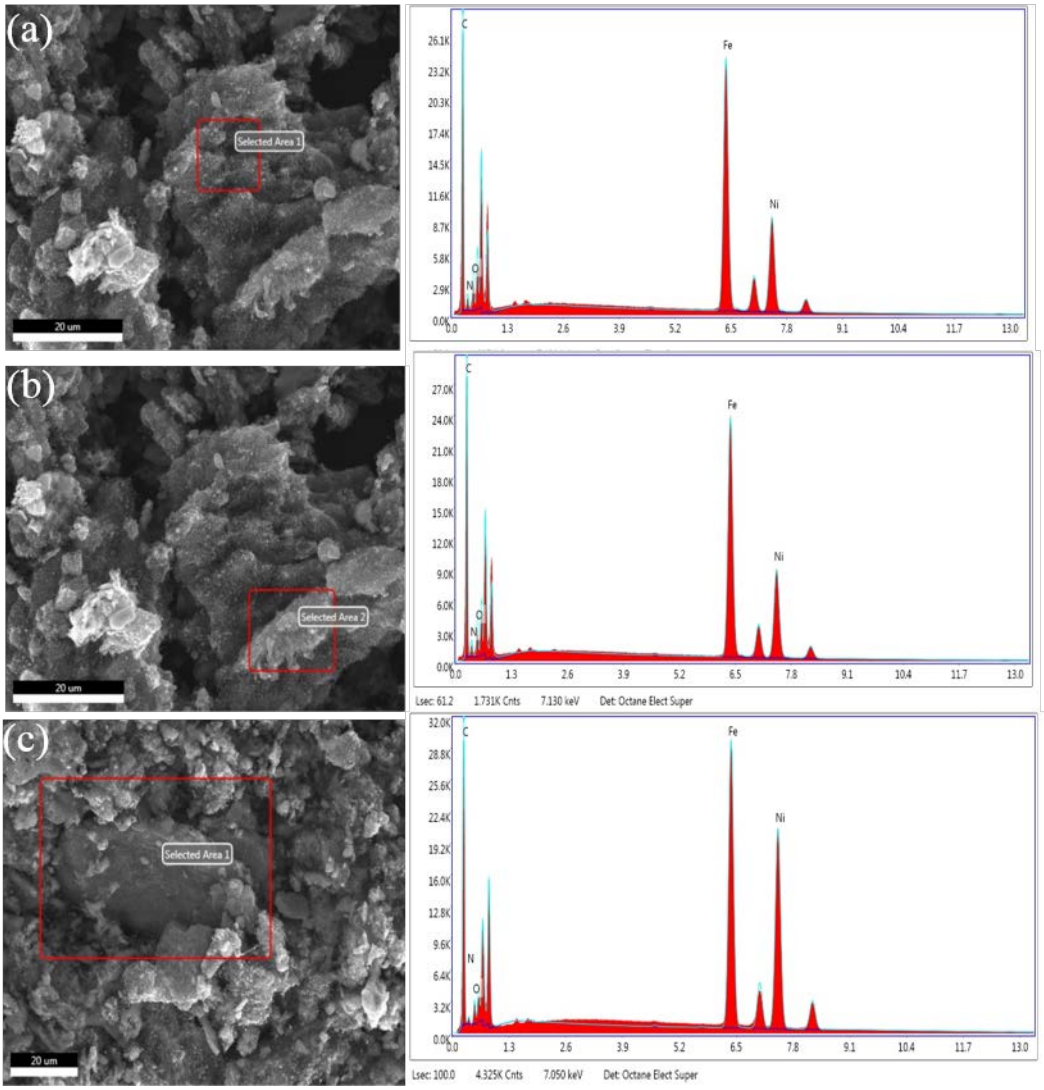


**Fig. S6** SEM images and compositions by SEM-EDS of $Fe_2Ni$-NCNT

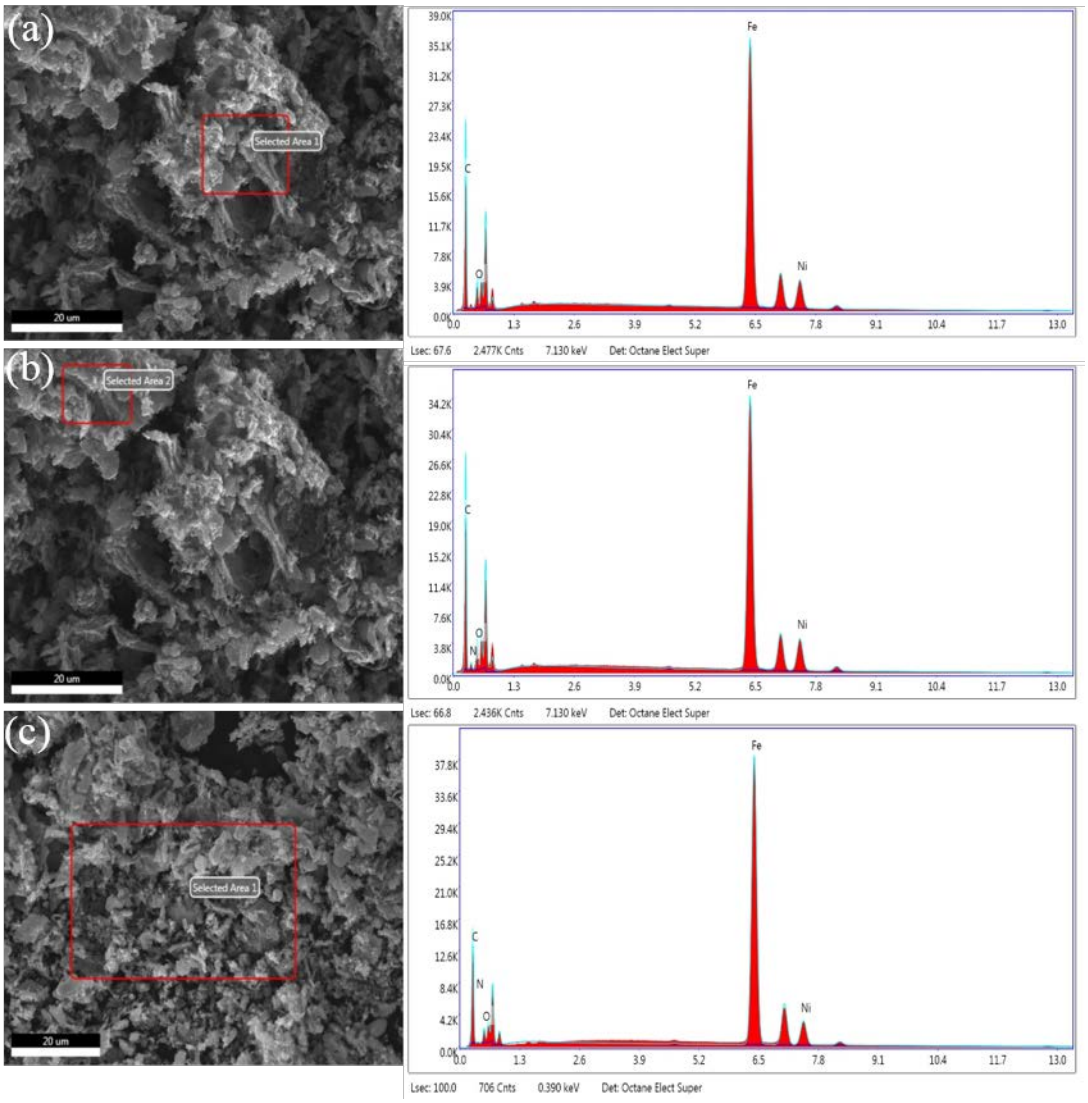


**Fig. S7** SEM images and compositions by SEM-EDS of $Fe_5Ni$-NCNT

**Table S1** Summary of compositions and ratio of M/Ni of $M_xNi$-NCNT samples by SEM-EDX

| Catalysts | Atomic composition % | | | | | | M/Ni Ratio | |
|---|---|---|---|---|---|---|---|---|
| | C | N | O | Fe | Co | Ni | Co/Ni | Fe/Ni |
| $Co_1Ni$-NCNT | 84.13 | 2.08 | 2.89 | — | 5.49 | 5.42 | 1.01 | — |
| $Co_2Ni$-NCNT | 86.22 | 1.72 | 3.23 | — | 5.96 | 2.87 | 2.08 | — |
| $Co_5Ni$-NCNT | 85.29 | 3.55 | 4.10 | — | 5.95 | 1.12 | 5.31 | — |
| $Fe_1Ni$-NCNT | 80.50 | 1.78 | 3.32 | 7.77 | — | 6.63 | | 1.22 |
| $Fe_2Ni$-NCNT | 71.26 | 4.86 | 4.50 | 12.74 | — | 6.66 | | 1.92 |
| $Fe_5Ni$-NCNT | 65.47 | 2.76 | 4.57 | 23.37 | — | 3.84 | | 6.08 |

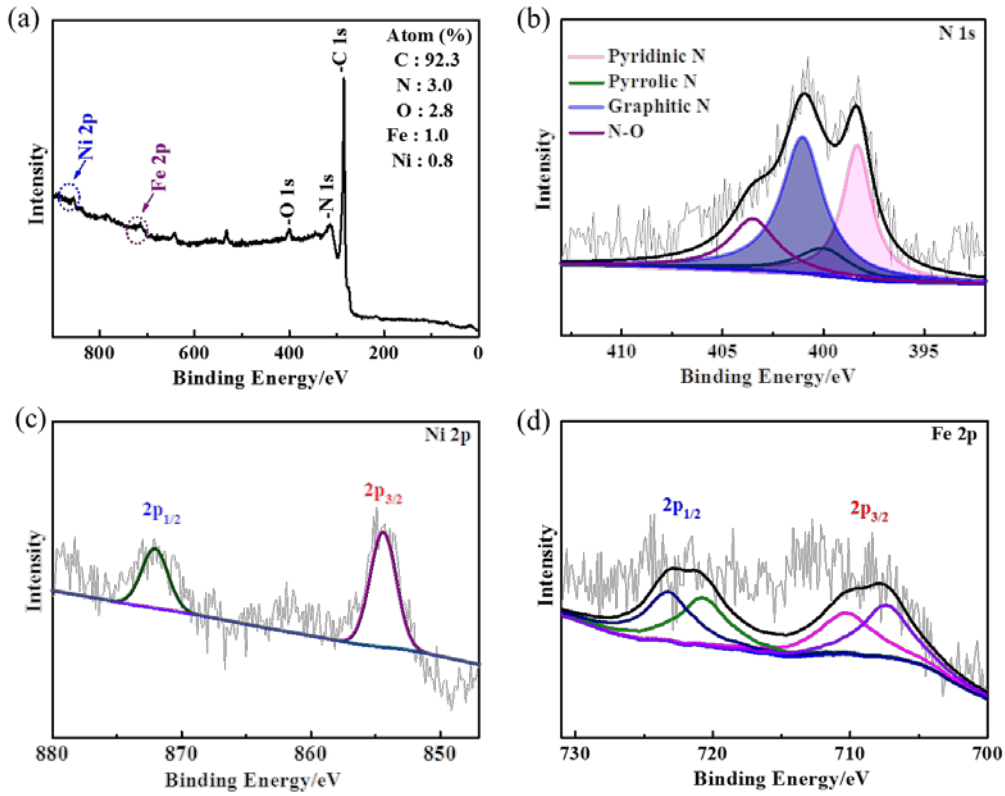


**Fig. S8** (a) XPS survey spectrum, the high-resolution XPS spectra of (b) N 1s, (c) Ni 2p, and (d) Fe 2p of $Fe_1Ni$-NCNT

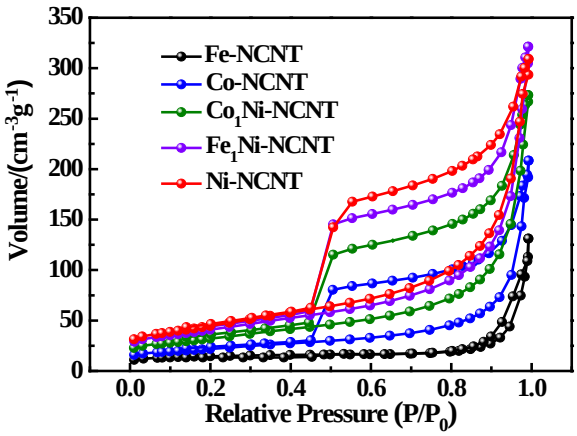


**Fig. S9** Nitrogen adsorption-desorption isotherms of various samples

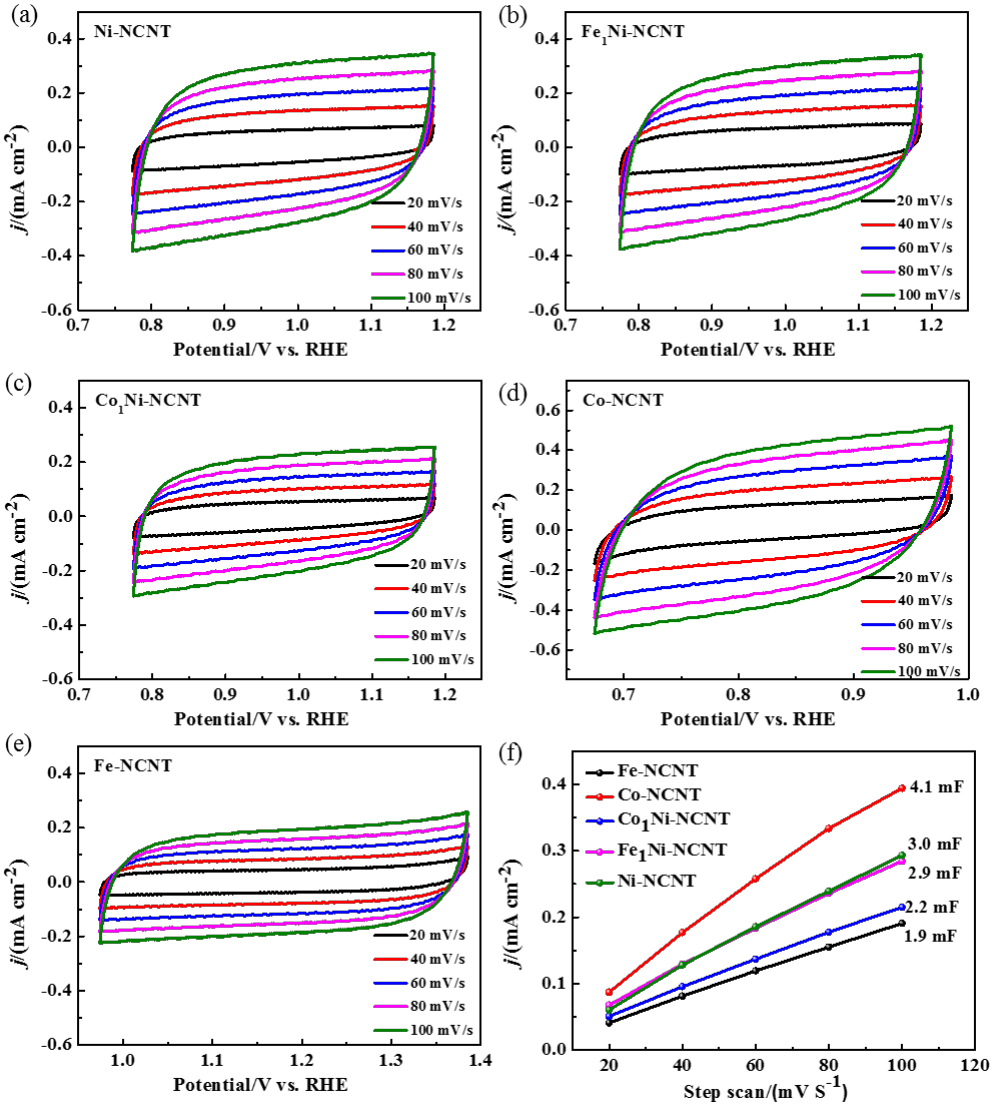


**Fig. S10** (a-e) Cyclic voltammograms at various scan rates for different samples. (f) The linear relationship between current density and scan rate.

**Linear sweep voltammetry (LSV) measurement**

Linear sweep voltammetry (LSV) measurement was conducted to evaluate the activity of samples in $N_2$-saturated 0.1 M $KHCO_3$ and then $CO_2$-saturated 0.1 M $KHCO_3$ at the scan of 50 mV/s. The potential range was 0 V ~ -1.2 V vs. RHE.

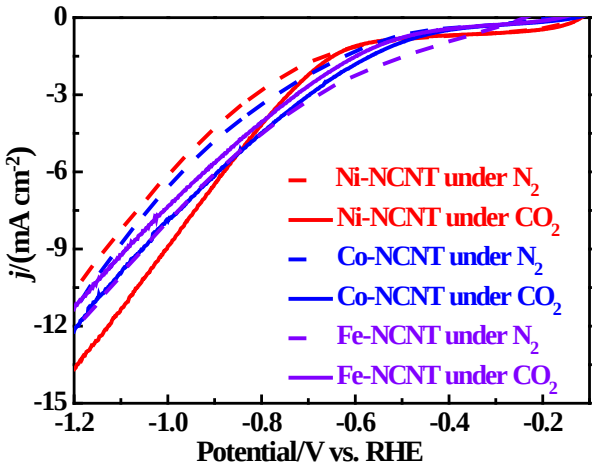


**Fig. S11** Linear sweep voltammetry curves of M-NCNTs in $CO_2$-saturated and $N_2$-saturated 0.1 M $KHCO_3$ at a scan rate of 50 mV/s

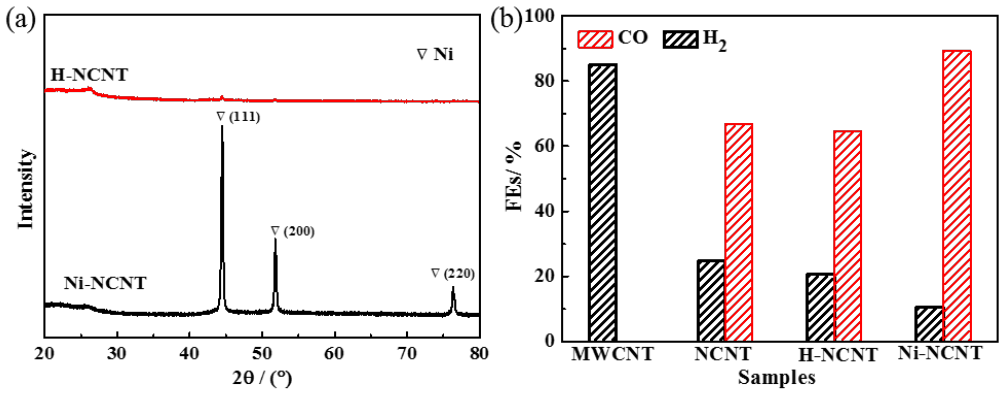


**Fig. S12** (a) XRD patterns and (b) FE of products at -1.0 V vs. RHE in $CO_2$ saturated 0.1 M $KHCO_3$ of various samples.

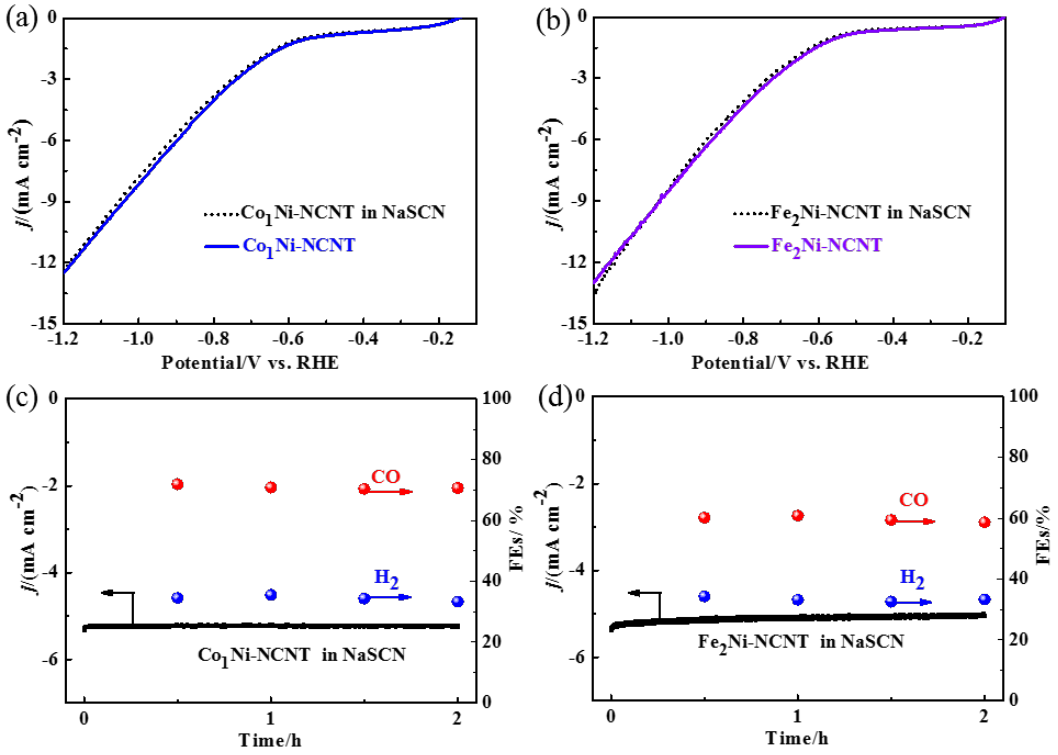


**Fig. S13** Linear sweep voltammetry curves of (a) $Co_1$Ni-NCNT, (b) $Fe_2$Ni-NCNT. Chronoamperometric I-t curve and $FE_{CO}$ and $FE_{H2}$ of (c) $Co_1$Ni-NCNT, (d) $Fe_2$Ni-NCNT at -1.0 V vs. RHE for Ni-NCNT poisoned with 20 mM NaSCN in $CO_2$ saturated 0.1 M $KHCO_3$

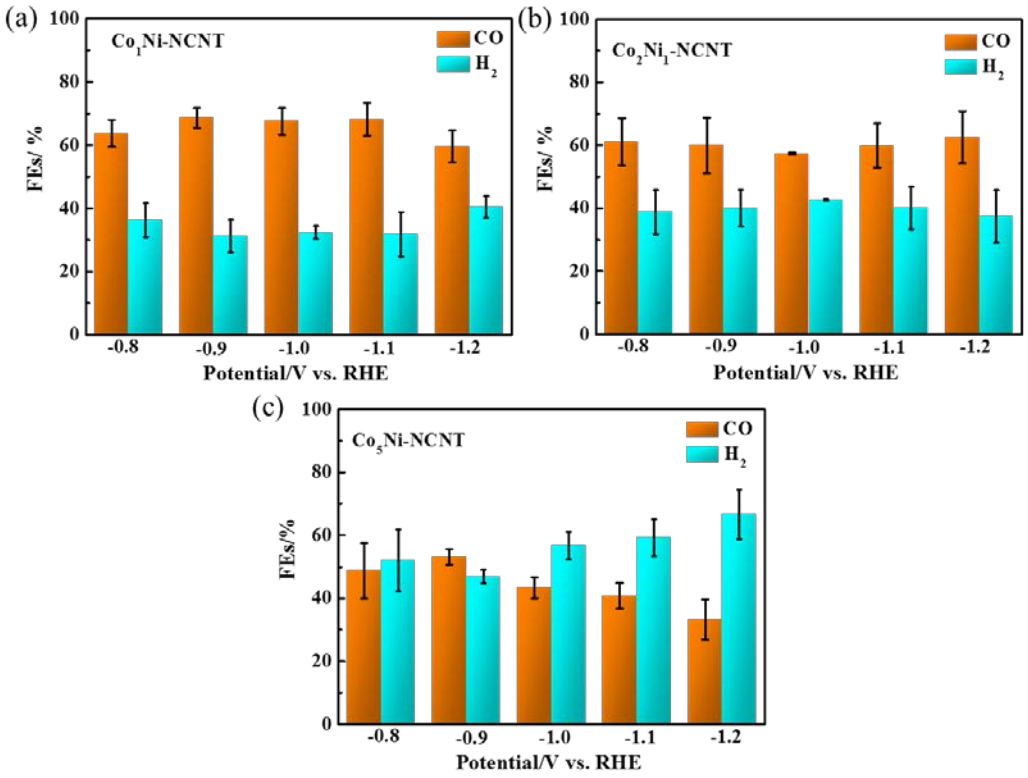


**Fig. S14** The faradaic efficiencies of CO and $H_2$ on (a) $Co_1Ni$-NCNT, (b) $Co_2Ni$-NCNT, and (c) $Co_5Ni$-NCNT at different potentials.

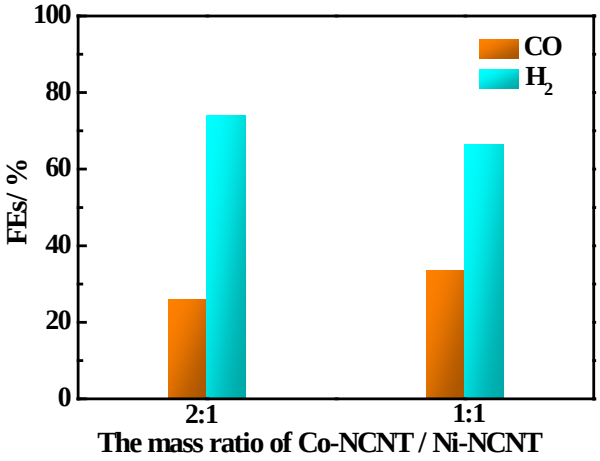


**Fig. S15** Faradaic efficiencies of various samples at -1.0 V vs. RHE

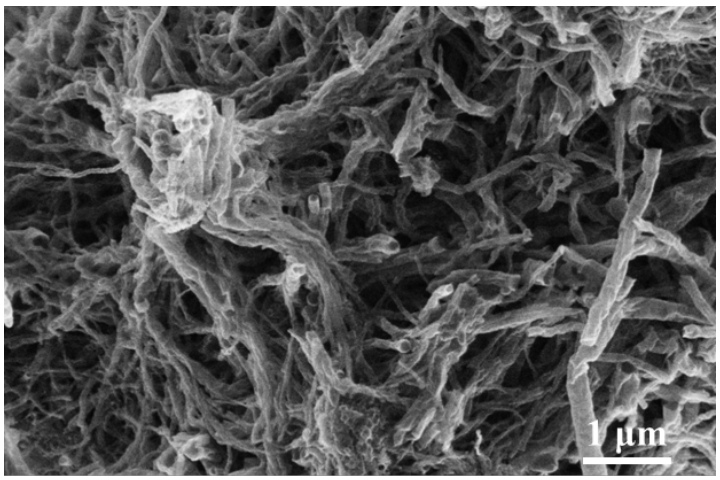


**Fig. S16** SEM image of $Co_1Ni$-NCNT electrode after 8h electrolysis at -1.0 V vs. RHE

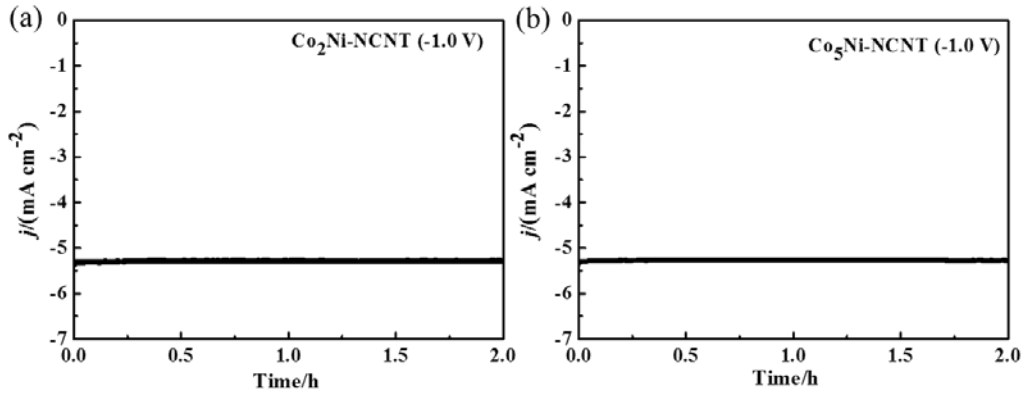


**Fig. S17** Long-term stability measurement of $Co_xNi$-NCNT at -1.0 V vs. RHE

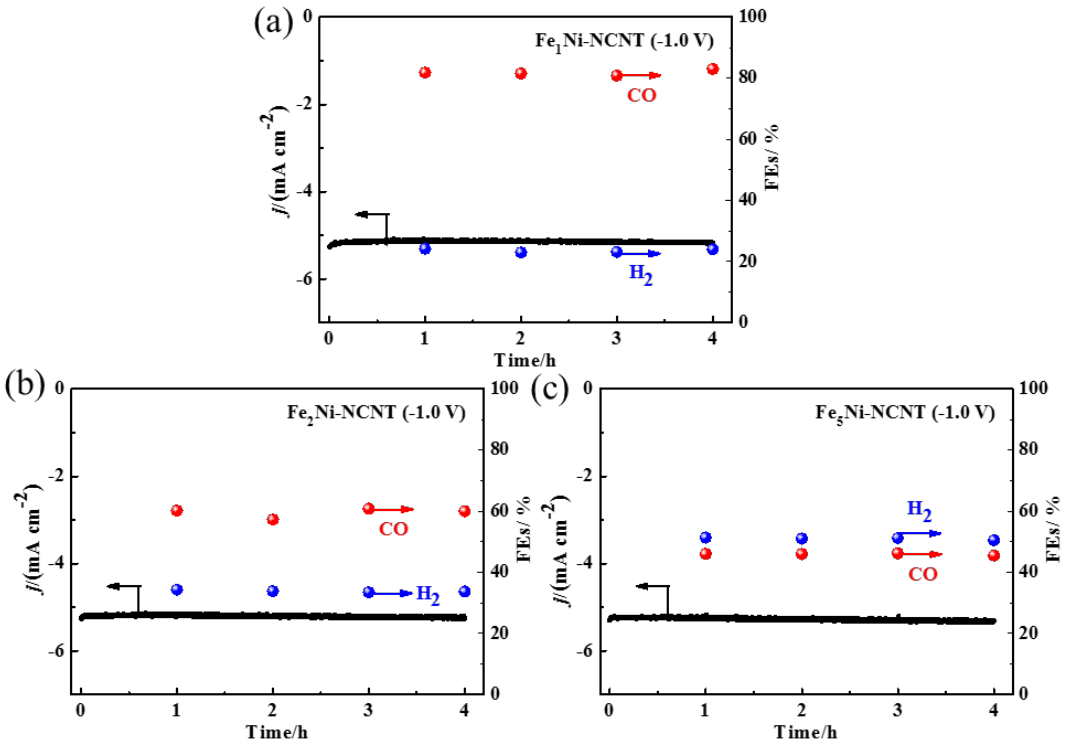


**Fig. S18** Total current density and Faraday efficiency of each product on (a) $Fe_1Ni$-NCNT, (b) $Fe_2Ni$-NCNT, and (c) $Fe_5Ni$-NCNT at -1.0 V vs. RHE in $CO_2$-saturated 0.1 M $KHCO_3$ solution.